

Fluorescent molecular rotor-based polymer materials for local microviscosity mapping in microfluidic channels

Dharshana Nalatamby, Florence Gibouin, Maxime Zitouni, Julien

Renaudeau, Gérald Clisson, Pierre Lidon, and Yaocihuatl Medina-Gonzalez*

Laboratoire du Futur, (LOF) - Syensqo - CNRS - Université de Bordeaux, UMR 5258, Bordeaux, 33600 Pessac, France.

Simon Harrisson

Univ. Bordeaux, CNRS, Bordeaux INP, LCPO, UMR 5629, Bordeaux, 33600 Pessac, France[†]

(Dated: February 19, 2025)

A viscosity-sensitive monomer consisting of a methacrylate-functionalized julolidone-based molecular rotor (MECVJ) was synthesized and used to obtain viscosity-sensitive polymers (poly(DMA-*s*-MECVJ)). The qualitative properties of the molecular rotor were preserved after its inclusion in the new polymer, in particular the effect of the viscosity of the surrounding medium on the fluorescence lifetime of the rotor. By grafting these polymers onto glass slides, viscosity-sensitive surfaces were obtained, showing good robustness in time after successive use and washing. As proof of concept, these surfaces were used to assemble a microfluidic chip capable of mapping viscosity of fluids flowing inside the channel.

I. INTRODUCTION

Viscosity is an intrinsic property of fluids, which determines the behavior of flows [1] and whose measurement can give important information about molecular composition and small-scale interactions. Consequently, viscosity measurement is essential in domains as varied as polymer synthesis and processing, crude oil processing, ink jet and 3D printing, cosmetic product formulation, slurries for battery fabrication and food processing. [2–5] In the medical domain, changes in viscosity may indicate the presence of pathological conditions [2, 6]. Mechanical rheometers or viscometers can be used to measure viscosity at the macroscale, but measurements at the microscale require specialized microviscometers that are prone to artifacts and some systems cannot be characterized with these tools. Other measurement techniques have been developed, for example electrochemical and electrokinetic microviscometers, but they may damage samples that are sensitive to heating or to the application of an electrical potential. Other techniques, designed for microfluidic and lab-on-a-chip applications, are based on the measurement of flow velocity under an imposed flow rate, and include capillary-driven flow microviscometers with vibrational, [7] thermal, [8] rotational [9] or optical detectors [10]. However, all of these approaches are not fully satisfactory to assess local variations of viscosity, as they all rely on averaged measurements over some volume, possibly small yet macroscopic.

Fluorescent molecular rotors (FMR) have recently been used as viscosity probes in systems that are not accessible to mechanical viscometers, including aerosols, [11] microfluidic channels, [12, 13] confined fluids [14] and living cells [15], enabling to map viscosity locally with excellent spatial resolution. After excitation by light, FMRs can undergo conventional radiative fluorescent decay, or non-radiative relaxation; the latter mode is accompanied by a twist and internal rota-

tion of the molecule. Interactions with the surrounding fluid hinder molecular rotation, favoring relaxation through the radiative path and increasing the observed fluorescence intensity and lifetime. As a result, these molecules are sensitive probes of local viscosity. After calibration of the fluorescence intensity or lifetime in fluids of known viscosity, FMRs can be used to determine the viscosity of unknown samples, and map spatial and temporal variations in the viscosity of complex systems. [12, 13, 16–18]. Some groups have used FMR to measure changes in viscosity during polymerization, [19] or to study the viscosity of a polymer around its glass transition temperature [20]. To date, FMRs have primarily been used in solution, with only a single report of the viscosity-responsive properties of 9-(2-carboxy-2-cyanovinyl)julolidine (CCVJ), a widely used FMR, immobilized on optical fibers [21]. The objective of the work presented here is to fabricate a viscosity-sensitive surface by grafting it with an FMR-functional polymer. The obtained viscosity-sensitive materials were incorporated into a microfluidic device to allow the measurement and mapping of the viscosity of fluids flowing through its channels. This strategy paves the way to a new generation of simple and affordable viscosity sensors for applications concerning microfluidics.

II. MATERIALS AND METHODS

All chemicals used were obtained from Sigma-Aldrich and used as received.

A. Synthesis of the viscosity-sensitive monomer (MECVJ)

A monomer, 9-2-(methacryloxyloxy)ethyloxycarbonyl-2-cyanovinyl-julolidine (MECVJ), was synthesized via condensation of an aldehyde and a methacrylate ester, which were themselves synthesized as described in the following paragraphs.

* yaocihuatl.medina-gonzalez@u-bordeaux.fr

[†] sharrisson@enscbp.fr

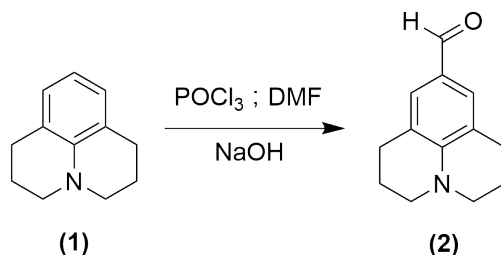


FIG. 1: Synthesis route of the julolidine aldehyde (2) from julolidine (1).

1. Synthesis of Julolidine Aldehyde

The protocol for the synthesis of the julolidine aldehyde was adapted from the work of Haidekker et al [22] (see Schema 1). Julolidine (0.5 g, 2.87 mmol) was placed in a mixture formed by 0.54 g (7.4 mmol) of N,N-dimethylformamide (DMF) and 7 mL (0.11 mol) of dichloromethane (DCM). Phosphorous oxychloride (POCl_3 , 0.58 mL (2.4 mmol)) was added dropwise. The mixture was stirred for 12 h at 25 °C. The flask was then placed in an ice bath for 15 min before adding 28 mL of an aqueous solution of sodium hydroxide (NaOH , 2 M). The mixture was stirred at 0 °C for 4 h.

$^1\text{H-NMR}$ was used to monitor the reaction advancement and to characterize the final product. These analyses were performed in a Bruker Avance III HD 400 spectrometer with a field frequency of 400.2 MHz. For this purpose, samples were dissolved in CDCl_3 at a concentration of about 10 – 12 mg mL^{-1} . Tetramethylsilane was used as internal standard at 0 ppm. Figure 17 shows the NMR spectra of julolidine and of the aldehyde. The characteristic peak for $-\text{CH}=\text{}$ band of julolidine can be observed at 6.53 – 6.57 ppm (t, ^1H) and the characteristic peak of aldehyde appears at 9.53 ppm (s, ^1H), which confirms the absence of julolidine in the final product. The purity of julolidine aldehyde was estimated at 97%. The peak at 5.52 ppm corresponds to traces of DCM used as solvent, which did not cause any problem for the next synthesis.

2. Synthesis of the Methacrylate Ester

The synthesis of the ester was performed through a modification of the work by Tsakos et al [23], who used 1-ethyl-3-(3-dimethylaminopropyl)carbodiimide hydrochloride (EDC) to induce the esterification. For that, 40 mL (0.8 mol) of acetonitrile and 2.9 g (24 mmol) of hydroxyethylmethacrylate (HEMA) were added to 2.8 g (42 mmol) of cyanoacetic acid and 6.3 g (33 mmol) of EDC. This reaction mixture was kept at 40 °C and stirred during 91 h, then acetonitrile was removed in a rotary evaporator. The obtained solid was dissolved in DCM and washed twice with 50 mL of HCl; then twice with 60 mL of water, twice with 60 mL of saturated sodium bicarbonate solution and once with 60 mL of saturated sodium chloride solution. The organic layer was obtained and dried with MgSO_4 . $^1\text{H-NMR}$ was used to verify the absence of by-products and of residual agents. DCM was evaporated under reduced pressure and the methacrylate ester was obtained as pale yellow

oil. The yield of this reaction was 77% and the purity of the final product was around 98%.

3. Synthesis of the viscosity-sensitive monomer (MECVJ)

The viscosity-sensitive fluorescent monomer, MECVJ was synthesized by the route shown in Schema 2. To this purpose, 0.51 g (2.57 mmol) of 2-cyanoacetoxyethylmethacrylate and 0.59 g (2.95 mmol) of julolidine aldehyde were added to 15 mL (185 mmol) of tetrahydrofuran. The mixture was kept at 50 °C and 1.6 mL (11.5 mmol) of triethylamine were added drop-wise. Stirring was continued for 96 h. The solvent was then evaporated at reduced pressure. The residue was recrystallized twice from a mixture of DCM/heptane (1:10), yielding a bright orange solid. The yield of this reaction was around 42% and the approximate purity of more than 95%. $^1\text{H-NMR}$ spectrum is shown in Figure S2.

B. Synthesis and characterization of viscosity-sensitive fluorescent polymers poly(DMA-*s*-MECVJ)

1. Synthesis

Four different polymers of different target molecular weights were synthesized, labeled from P1 to P4 as shown in Table I. The initiator used was azobisisobutyronitrile (AIBN). The required amounts of monomers, initiator [I] and RAFT agent were calculated to obtain the desired ratio of equivalent numbers as $[\text{MECVJ}]/[\text{DMA}]/[\text{I}]/[\text{RAFT}]$. For instance, for P3, 31.9 mg (0.10 mmol) of RAFT agent and 3.8 mg (0.023 mmol) of AIBN were added to 9 mL (106 mmol) of dioxane in a twin-neck round bottom flask. Then, 994 mg (10.03 mmol) of DMA and 38.9 mg (0.137 mmol) of MECVJ were added to the flask. The reaction medium was then degassed by bubbling with N_2 during 30 min. The flask was heated to 60 °C and stirred to start the polymerization reaction. To monitor the conversion of MECVJ and DMA, samples for $^1\text{H-NMR}$ analyses were obtained via cannula transfer under a current of N_2 . Quenching of the polymerization was obtained by immersion of the flask in an ice bath. Removal of dioxane under reduced pressure afforded a dark yellow viscous liquid, which was solubilized in 10 mL of DCM and added drop-wise to 200 mL of diethyl ether. Precipitation of the polymer was

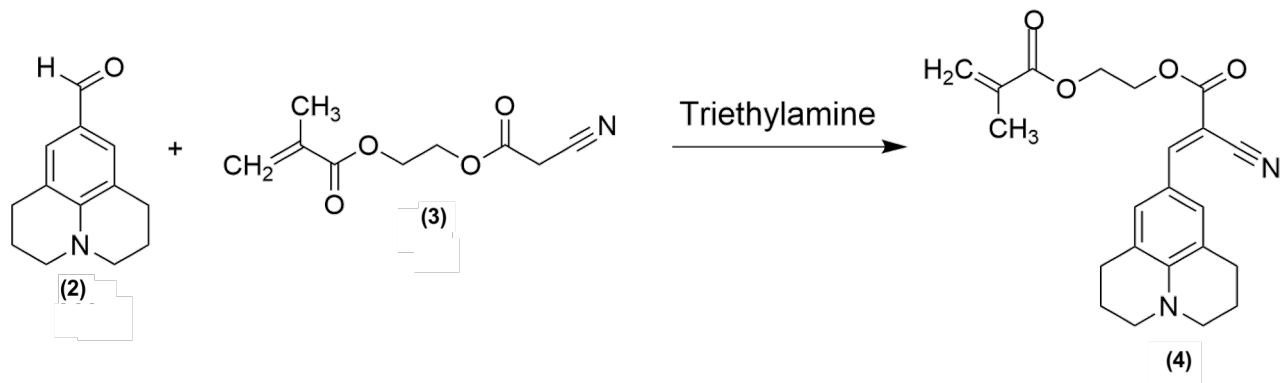


FIG. 2: Synthesis route of MECVJ (4) via the condensation of julolidine aldehyde (2) and methacrylate ester (3).

then observed. Centrifugation at 2500rpm and at 5°C during 30 min allowed to obtain a dark orange solid.

2. Characterization of the poly(DMA-*s*-MECVJ)

a. NMR $^1\text{H-NMR}$ spectroscopic analyses were performed with a Bruker Avance III HD 400 spectrometer with a field frequency of 400.2 MHz. The analyzed polymers were dissolved in approximately 0.5 mL of CDCl_3 , and the concentration of the polymer solutions was 10-12 mg mL^{-1} . The samples were referenced to TMS (0 ppm).

b. Size Exclusion Chromatography (SEC) Polymer molar masses were determined by SEC using N,N-dimethylformamide (DMF + LiBr 1g/L) on an Ultimate 3000 system from ThermoFischer Scientific (Ilkirch, France) equipped with a differential refractive index detector from Wyatt technology (Santa Barbara CA, USA). Polymers were separated on three Shodex Asahipack gel columns [GF 310 (7.5×300 mm), GF510 (7.5×300 mm), exclusion limits from 500 – 300000 Da] at a flowrate of 0.5 mL min^{-1} . The column temperature was held at 50°C. An Easivial™ kit of Polystyrene from Agilent (Santa Clara CA, USA) was used as calibration standard (M_n from 162 to 364000 Da) to provide polystyrene-equivalent molecular weights.

C. Characterization of response to viscosity

In order to quantify the response of MECVJ and poly(DMA-*s*-MECVJ) to the viscosity of the surrounding medium, solutions of these FMR were prepared in DMSO/glycerol mixtures. For that, stock solutions of MECVJ and of poly(DMA-*s*-MECVJ) in DMSO were prepared beforehand, and dispersed in DMSO-glycerol mixtures. Care was taken to keep a similar concentration of FMR in all solutions, equal to $10^{-5} \text{ mol L}^{-1}$, in order to avoid bias on fluorescence intensity due to changes of concentration.

D. Viscosity measurements

In order to determine viscosity, ramps of shear rate were applied to the solution by using a Kinexus Ultra+ rheometer (Netzsch). Samples of low viscosity (below 15 mPas) were analyzed using a double-gap geometry whereas cone-plate geometry was used for viscous samples (above 15 mPas). A Peltier module was used to regulate the experimental temperature, which was fixed at 25°C.

Both for solutions of MECVJ and of polymer poly(DMA-*s*-MECVJ), viscosity was found to be independent on shear rate. This Newtonian behavior for polymer solution is not surprising as the added polymer is strongly diluted. The average over all of the applied shear rates was taken as the final viscosity value.

1. Photophysical characterization

For the different solutions, absorption and emission spectra were measured using a Cary UV-Vis spectrophotometer and a Cary Eclipse Fluorescence spectrophotometer both from Agilent Technologies. Fluorescence intensities I_F were measured as the maximum value in emission spectra.

Lifetimes τ_F were measured using a LIFA system for Fluorescence Lifetime Imaging Microscopy (FLIM) from Lambert Instruments, equipped with a LED source of wavelength 451 nm, close to the maximum of absorption of the FMR. This instrument allows the mapping of fluorescence lifetimes across the field of view of a microscope. The lifetimes τ_F of the samples were measured by recording a reference beforehand; a fluorescein aqueous solution ($10 \mu\text{mol L}^{-1}$, Sigma-Aldrich 46955-1G-F) prepared in pH 10 buffer solution with tabulated lifetime $\tau_{\text{ref}} = 4.02 \text{ ns}$. FLIM acquisitions were carried out using a modulation frequency of $f = 40 \text{ MHz}$ and 12 acquisition phases with a $1 \times \text{CCD}$ gain, ensuring maximum resolution.

	n_{targeted}	DMA/MECVJ (mol %:initial)	t (h)	Conv.DMA (%)	$M_n^{\text{[SEC]}}$ (g mol ⁻¹)	$M_n^{\text{[theor]}}$ (g mol ⁻¹)	\mathcal{D}
P1	20	100/1	27	93	4575	2219	1.19
P2	50	95/5	16	85	3697	5270	1.21
P3	100	100/1	6	81	9240	8645	1.18
P4	100	90/10	54	81	4742	11346	1.76

TABLE I: Details of the four poly(DMA-*s*-MECVJ) statistical copolymers synthesized at 60°C and their macromolecular characteristics. The total number of monomers (MECVJ and DMA) targeted in a polymer chain is denoted as n_{targeted} , t is the polymerization reaction time in hours. The conversion of DMA (%) was determined from ¹H-NMR. Masses $M_n^{\text{[SEC]}}$ and $M_n^{\text{[theor]}}$ are polystyrene equivalents, determined by SEC in DMF/LiBr, calibrated using polystyrene standards. \mathcal{D} is the polydispersity index.

2. Förster-Hoffmann model

The relationship between fluorescence intensity I_F and lifetime τ_F of FMR, and viscosity η is commonly described by a power-law relation [12]. Briefly, the relationship between the quantum yield (ϕ_F) of a molecular rotor and the viscosity of the surrounding medium can be simplified into an expression called the Förster-Hoffman equation [18, 24]:

$$\log \phi_F = \alpha \log \eta + C \quad (1)$$

in which α is a constant usually dependent on the rotor and C is a proportionality constant. As I_F and τ_F are proportional to ϕ_F , the Förster-Hoffman expression can then be rewritten as :

$$\log I_F = \alpha \log \eta + C_{I_F} \quad (2)$$

and :

$$\log \tau_F = \alpha \log \eta + C_{\tau_F}. \quad (3)$$

While coefficients C_{I_F} and C_{τ_F} are difficult to interpret and depend on instrumental factors, the coefficient α , which corresponds to the exponent of the power-law, is expected to be similar for both parameters I_F and τ_F and quantifies the sensitivity of the FMR to the surrounding viscosity. Equations (2) and (3) were thus used to analyze the response of FMR.

Equation (3) is particularly valuable for applications, as τ_F is independent of the local concentration of the rotor and of other instrument-related factors such as local light intensity. It can thus be used for viscosity measurements of unknown samples provided a prior calibration has been established using similar fluids of known viscosities.

E. Grafting of poly(DMA-*s*-MECVJ) materials to glass surfaces and its use in microfluidics devices fabrication

A "grafting-to" strategy based on the work by Duwez et al [25] was adopted for the grafting of the viscosity-sensitive polymers, poly(DMA-*s*-MECVJ), to glass surfaces. For that, a thin film of gold of 30nm was deposited on a glass slide by metal evaporation with a pressure of 10⁻⁶ mbar in a glove box. A chromium film of 5nm of thickness was prior deposited onto the glass slide to ensure a good adhesion of the gold. A solution of polymer in water (14.3 mgL⁻¹) was deposited

onto the gold-coated glass slide, and left in a closed Petri dish at room temperature for at least 16h. This step was carried out in the dark to prevent possible photobleaching. The glass slide was then rinsed with 10mL of distilled water and dried with N₂.

To qualitatively confirm the grafting of poly(DMA-*s*-MECVJ), contact angle measurements were performed using the sessile drop method using the Attension Theta Optical Tensiometer, as changes of hydrophilicity would confirm the presence of polymers on the glass slide.

To further analyze grafting efficiency, XPS analyses were performed by using a VG ESCALAB 220i-XL X-ray photoelectron spectrometer with non-monochromatic MgK α radiation ($h\nu = 1253.6\text{eV}$) and a pass energy of 80eV. An internal reference of C1s binding energy (285.0eV) was used. The lateral resolution of the setup was of 150 μm in routine in ultra-high vacuum conditions at 10⁻⁸ mbar. These XPS analyses were performed on surfaces grafted from a solution of 5mgL⁻¹ of polymer in water. Fluorescence properties of the prepared surface were measured with the FLIM-LIFA.

A viscosity-sensitive microfluidic chip prototype was then fabricated, as schematized in Figure 3 . Using standard soft lithography techniques, a straight microfluidic channel of 2mm of width and 100 μm of height was patterned in a PDMS block. This block was then sealed by clamping it with a glass slide grafted with poly(DMA-*s*-MECVJ). The response of the surface was calibrated with DMSO/glycerol solutions of known viscosity and Förster-Hoffman model was applied to the obtained responses. Then, as a proof of concept, the response obtained by using the microfluidic channel was studied for different fluids as follows. Two different water/glycerol solutions of different viscosities, respectively of 2mPas and 843mPas, were alternatively injected, with time period long enough to ensure the injected fluid flushed the previous one.

III. RESULTS AND DISCUSSION

A. Photophysical properties of the viscosity-sensitive monomer MECVJ

The absorption and emission maxima of the monomer MECVJ were found at 467nm and 508nm respectively as shown in Figure 4a, similar to what was reported for

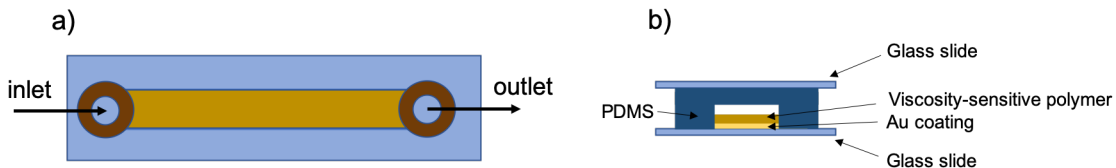


FIG. 3: Schematics of the viscosity-sensitive microfluidic chip fabricated (not at scale), a) top view, b) side view.

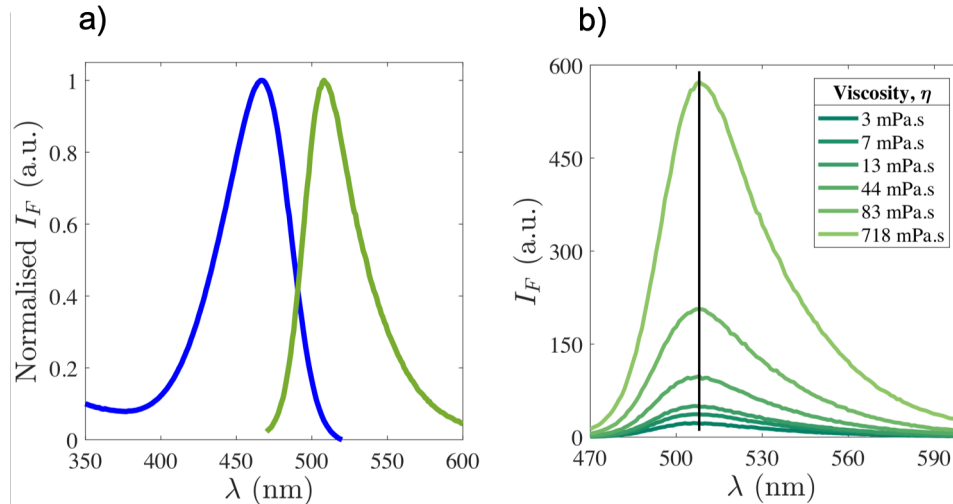


FIG. 4: a) Excitation and emission spectra of MECVJ in glycerol, b) Emission spectra of MECVJ in DMSO-glycerol mixtures. The black solid line was added to indicate the unchanged maxima of the emission spectra with polarity of the solution.

julolidine-based FMR, meaning that the fluorescence properties were not affected by the addition of the methacryloyloxyethyl group to the (cyano-vinyl) julolidine base. The polymers were tested in a variety of DMSO-glycerol mixtures, of varying viscosity and polarity without changes in the maximum wavelengths of absorption and emission (Figure 4b), which supports the fact that MECVJ is not sensitive to the polarity of the medium, while maximum intensity I_F increases with viscosity.

Figure 5 shows the fluorescence intensity I_F and fluorescence lifetime τ_F of MECVJ as function of viscosity. The Förster-Hoffman model was found to be valid in the range of viscosity used for calibration. The coefficient obtained ($\alpha = 0.6$) was similar to those reported for other julolidine-based FMR, such as DCVJ in glycerol/ethylene glycol mixtures of different viscosities [26, 27]; values obtained for C parameter were $C_{I_F} = 1.1$ and $C_{\tau_F} = -2.1$ when η is expressed in mPa.s and τ in ns.

B. Synthesis and characterization of the viscosity-sensitive copolymer poly(DMA-*s*-MECVJ)

1. Synthesis of poly(DMA-*s*-MECVJ)

The viscosity-sensitive copolymers were synthesized using RAFT (reversible addition-fragmentation chain transfer)

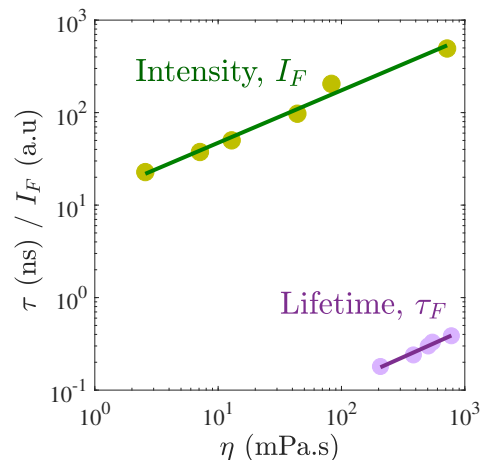


FIG. 5: MECVJ fluorescence intensity (I_F) and lifetime (τ_F) as function of the viscosity (η) of the surrounding media. Solid lines are respectively powerlaw fits along Eq. (2) and (3).

polymerization [28]. They contained 1-10% of MECVJ and 90-99% of dimethyl acrylamide (DMA), and had targeted degrees of polymerization ranging from 20 to 100. DMA was chosen as its polymer is soluble in a wide range of po-

lar and nonpolar solvents, ensuring that the copolymerized MECVJ units would be accessible to the solvents that are to be analyzed. An additional benefit of using an acrylamide comonomer is that acrylate and acrylamide monomers are consumed less rapidly than methacrylates in copolymerization [29, 30]. This ensures near-quantitative conversion of the MECVJ even when full conversion of the DMA is not reached, reducing the risk of contamination of the copolymer with unreacted MECVJ.

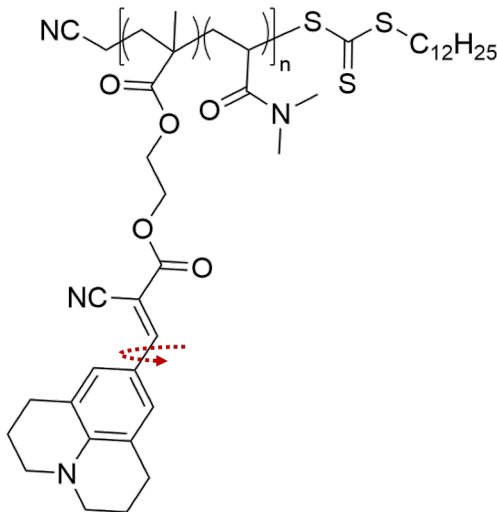


FIG. 6: General structure of the targeted viscosity-sensitive polymer, poly(DMA-*s*-MECVJ). The dotted arrow shows the intended rotation of the julolidine part.

The evolution of MECVJ and DMA polymerization for P2 is shown in Figure 7. MECVJ can be seen to be fully incorporated into the copolymer before full conversion of DMA is reached, with the absence of two characteristic proton peaks of MECVJ at 5.5 and 6.1 ppm after 13 hours of reaction.

The quality of the retrieved polymers was analyzed with $^1\text{H-NMR}$ and SEC, and the results obtained for P3 are portrayed in Figure 8. An absence of starting monomers and solvent can be perceived, and the narrow differential refractive index signal in the chromatogram confirms the low dispersity of the synthesized polymer. Nevertheless, as listed in Table I, a low dispersity value was not achieved for P4, for which MECVJ makes up around 10% of its composition. Cyanomethyl dodecyl trithiocarbonate is a mediocre RAFT agent for methacrylate monomers, it could be that there was too much MECVJ in this polymerization, and thus, control was lost. However, it would be more likely that the fluorescent part of the MECVJ interacts with the propagating radicals in some way. Lower than expected molecular weights and higher than expected dispersities may indicate irreversible chain transfer reactions, while retardation may indicate increased chain termination. This reasoning could explain the lower than expected molar masses M_n obtained for P2 and P4.

At the end of the synthesis, the polymers obtained after precipitation contained no detectable unreacted MECVJ or DMA. SEC analyses indicated that some control over molec-

ular weight was obtained, as polymers with a higher ratio of RAFT agent to monomer displayed lower molecular weights. Reasonable agreement between the experimental molecular weight and the theoretical molecular weight, calculated from the conversion of each monomer, as well as relatively narrow molecular weight distributions ($\mathcal{D} \approx 1.2$) were observed for P2 and P3. Higher than expected molecular weight, combined with low dispersity, was obtained for the polymer with the lowest targeted molecular weight (P1), which may indicate some fractionation during precipitation leading to loss of the lowest molecular weight fraction of the polymer. The polymer with the highest concentration of MECVJ (P4) exhibited a broad molecular weight distribution and lower than expected M_n , suggesting that significant termination occurred during this polymerization. The loss of control of the polymerization may be due to interactions between MECVJ and the propagating radicals, leading to irreversible chain transfer or other chain-terminating reactions.

2. Photophysical properties of poly(DMA-*s*-MECVJ)

The absorption and emission maxima were obtained for the synthesized polymers (see Figure 9) and found to be similar to the wavelengths obtained for MECVJ in solution. Absorption and emission wavelengths for the different synthesized polymers are gathered in Table II.

Polymer	$\lambda_{\text{absorption}}$ (nm)	$\lambda_{\text{emission}}$ (nm)
P1	465	504
P2	461	510
P3	461	506
P4	458	506

TABLE II: Absorption and emission maxima of different poly(DMA-*s*-MECVJ) synthesized in this work.

Figure 10 shows the variations obtained in fluorescence emission spectra of the different polymers as function of the viscosity of the surrounding medium. The obtained results were in overall agreement with those obtained for the MECVJ, which confirmed that the fluorescence properties are maintained after polymerization. The length of the polymer chain did thus not hinder the response of the polymer and the wavelength of maximum emission of the polymers was independent of the viscosity of the samples.

As for MECVJ, it was observed that the emission wavelength is similar in the different solutions, which confirmed that fluorescent emission is not affected by the polarity of the solution, and that only viscosity influenced the quantum yield ϕ_F of these polymers and hence their lifetime τ_F .

Double logarithmic plots of fluorescence intensity and lifetime as function of viscosity are shown in Figure 11. The Förster-Hoffman relationship was found to be valid for the polymers synthesized in the range of viscosities tested. More precisely, comparable yet smaller α coefficients were found for polymers in comparison with free MECVJ, indicating

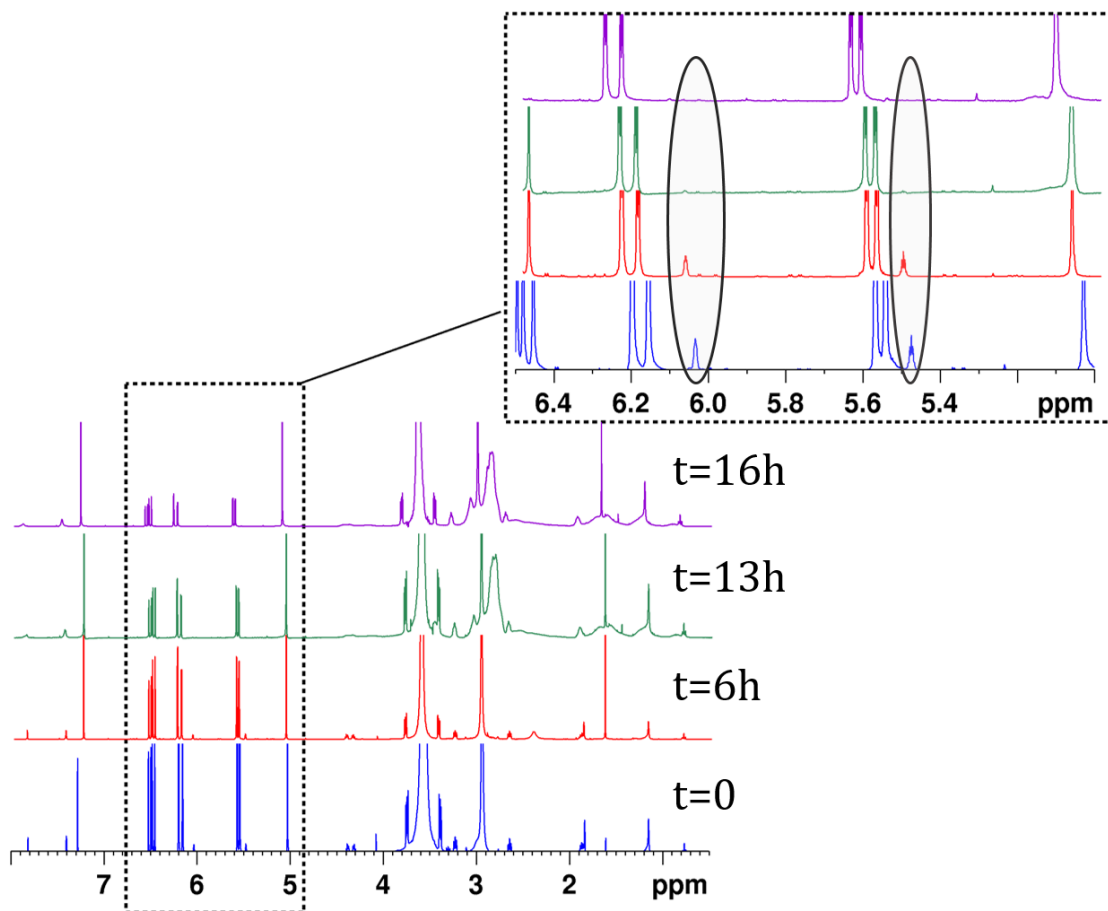


FIG. 7: ^1H -NMR monitoring during the synthesis of poly(DMA-*s*-MECVJ), P2, in CDCl_3 . The inset zoomed spectra focus on the over-time disappearance of the characteristic peaks of MECVJ.

lower sensitivity of the polymers to viscosity. At high concentration of MECVJ, for polymers P2 and P4, a discrepancy was observed between the coefficients α measured for intensity and for lifetime which could arise from a multi-exponential decay behavior of the polymers fluorescence, reflected in the lifetime measurements but not in the intensity measurements [31].

Although the polymers were slightly less sensitive to viscosity than the monomer, they could still be proposed for quantitative measurement purposes and allowed to prepare viscosity-sensitive surfaces. Moreover, the lifetime values measured for the polymers were longer than these obtained for MECVJ; this phenomenon arises from the rigidity of MECVJ when it is integrated in the poly(DMA-*s*-MECVJ), which favors the emissive relaxation pathway, increasing as well the time that the FMR stays in the excited state and consequently τ_F . This can be an advantage in the case of low viscosity solutions, associated with lifetime below the resolution limit of the FLIM. For instance, given the resolution limit of the LIFA equipment (limited to lifetime $\tau_F > 0.15\text{ ns}$), MECVJ could be used to measure viscosities larger than 200 mPas, while the use of the polymers allowed to test viscosities ten times lower.

C. Grafting of poly(DMA-*s*-MECVJ)

1. Quality of grafting and sensitivity to viscosity

After grafting the polymer onto the gold-coated glass surfaces, contact angles decreased from around 70° to around 30° , as the polymer increased the hydrophilicity of the surface. The XPS spectra for a surface obtained by grafting P3 are shown in Figure 12. The increase of the atomic percentage of carbon and oxygen, the decrease in the atomic percentage of gold and the appearance of chemisorbed sulfur at 162.4 eV were attributed to the presence of grafted polymer [32]. No leaching of the polymer was observed after thoroughly washing the surface with water. After grafting, polymer P4 afforded the best surface, in terms of homogeneity and of fluorescence response.

Drops of various water/glycerol mixtures of different viscosities were deposited onto the surface obtained after grafting of P4. The excitation wavelength was set at 451 nm in the FLIM-LIFA and fluorescence lifetimes for each solution were recorded. The results obtained are shown in Figure 13. Figure 13a shows the response of lifetime τ_F to mixtures of different viscosities for different grafting times. After contin-

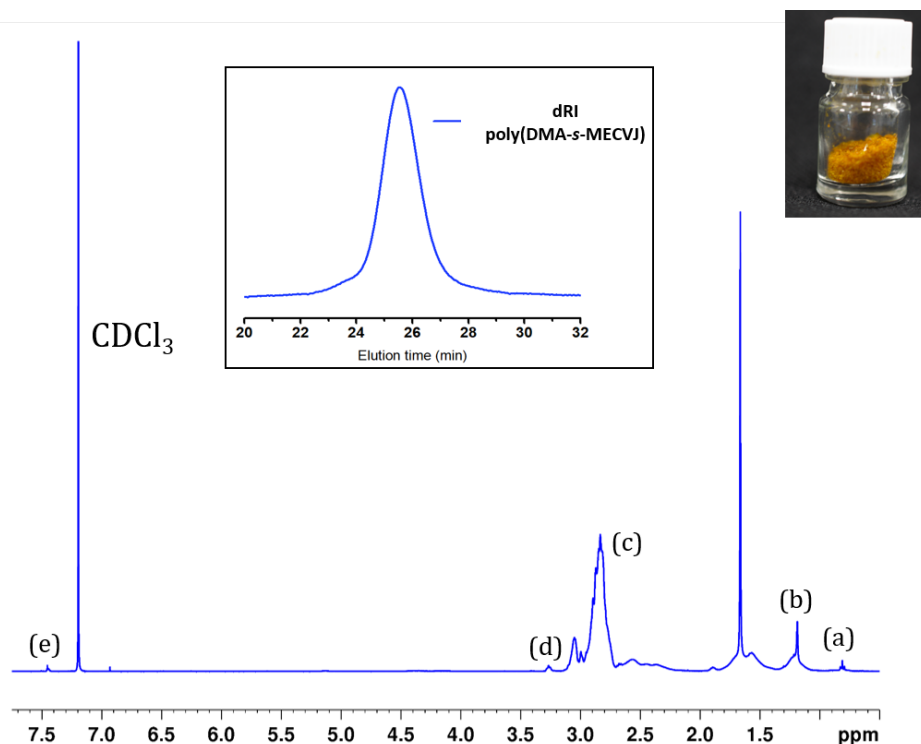


FIG. 8: $^1\text{H-NMR}$ spectra of poly(DMA-*s*-MECVJ) P3. (a), (b), and (d) represent the characteristic proton peaks of the RAFT agent, (c) the polymerized DMA, and (e) the polymerized MECVJ. The inset chromatogram obtained via SEC in DMF represents the differential refractive signal of the copolymer. Top-right inset: an image of P3 synthesized in this work.

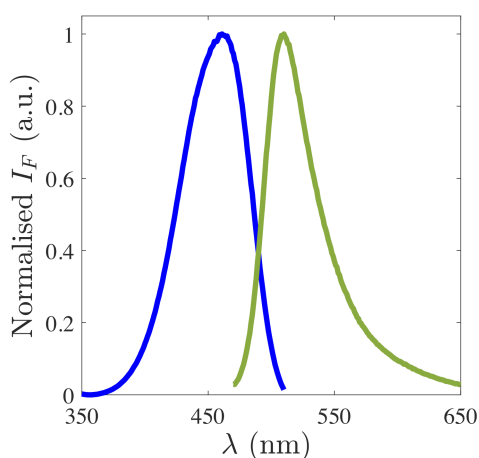


FIG. 9: Absorption (blue line) and emission (green line) spectra of P2 in glycerol. Maximum of absorption and emission are respectively 461 nm and 510 nm.

uous washing for 63 h, grafted surfaces still shown satisfactory response to viscosity of flowing solutions (Figure 13b), indicating that the polymer was robustly grafted.

Coefficient α for grafted polymers was decreased compared to polymer in solution, reaching values around 0.1. De-

spite this important loss of sensitivity to viscosity after grafting, it remained sufficient to fabricate viscosity-sensitive surfaces and consider to design a microfluidic chip capable of measuring the viscosity of a fluid flowing through it.

2. Towards a viscosity-sensitive microfluidic chip

As a proof of concept, the obtained surface with grafted polymers was used to prepare the device shown in Figure 14.

Figure 15a shows the variation of lifetime τ_F measured for different mixtures of water-glycerol of varying viscosity using the FMR-integrated microfluidic chip developed in this work. In order to check the repeatability of the process, the experiments were repeated with two chips prepared following the same protocol. The viscosity-sensitivity of the polymeric surface was thus not modified by its integration into the microfluidic device.

The dynamic response of the developed microfluidic device to viscosity was further investigated, as depicted in Figure 15b. The response of the polymer-grafted microfluidic chip during the injection of the $\eta \approx 2$ mPas (lower-viscosity) solution was measured before the injection of the 843 mPas (high-viscosity) solution at time (a). Time (b) marks the end of the injection of high-viscosity fluid, and at time (c), the lower-viscosity fluid was reintroduced into the microchannel. For both fluid injections, after a delay related to the time required by the fluid to reach the observation area, variations

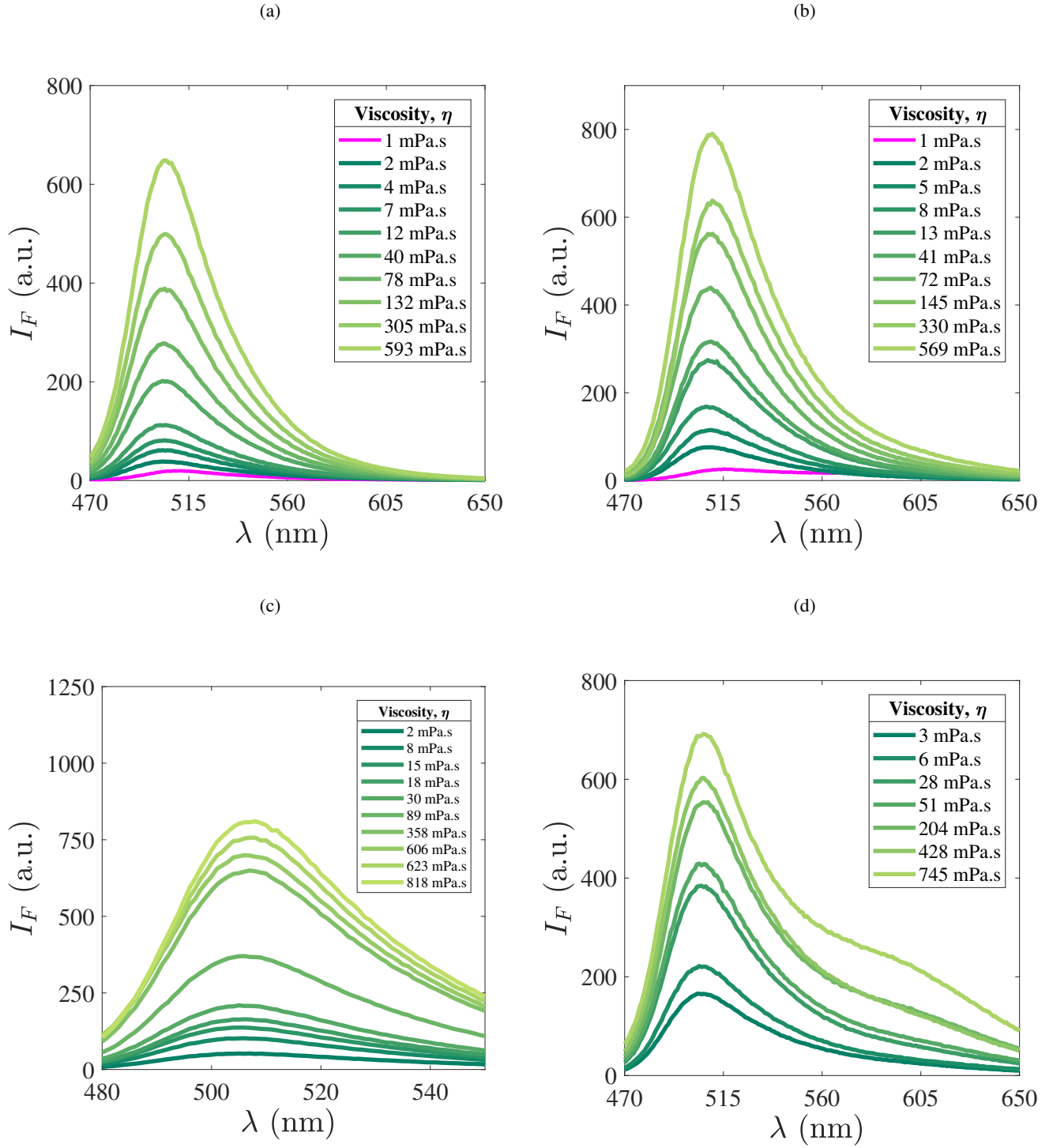


FIG. 10: Emission spectra of (a) P1, (b) P2, (c) P3, and (d) P4 in different mixtures of varying viscosity.

of lifetime τ_F were observed, consistently with the expected viscosity changes.

The response of the chip to the viscosity of the different fluids injected shows the satisfactory response of the polymer to the viscosity of the fluids flowing through the chip. Figure 16a

shows the successive lifetimes τ_F obtained at a fixed position in the microchannel by switching back and forth the injection between two different water/glycerol mixtures.

It is worth highlighting that the values of τ_F obtained for the tested mixtures did not change throughout seven successive

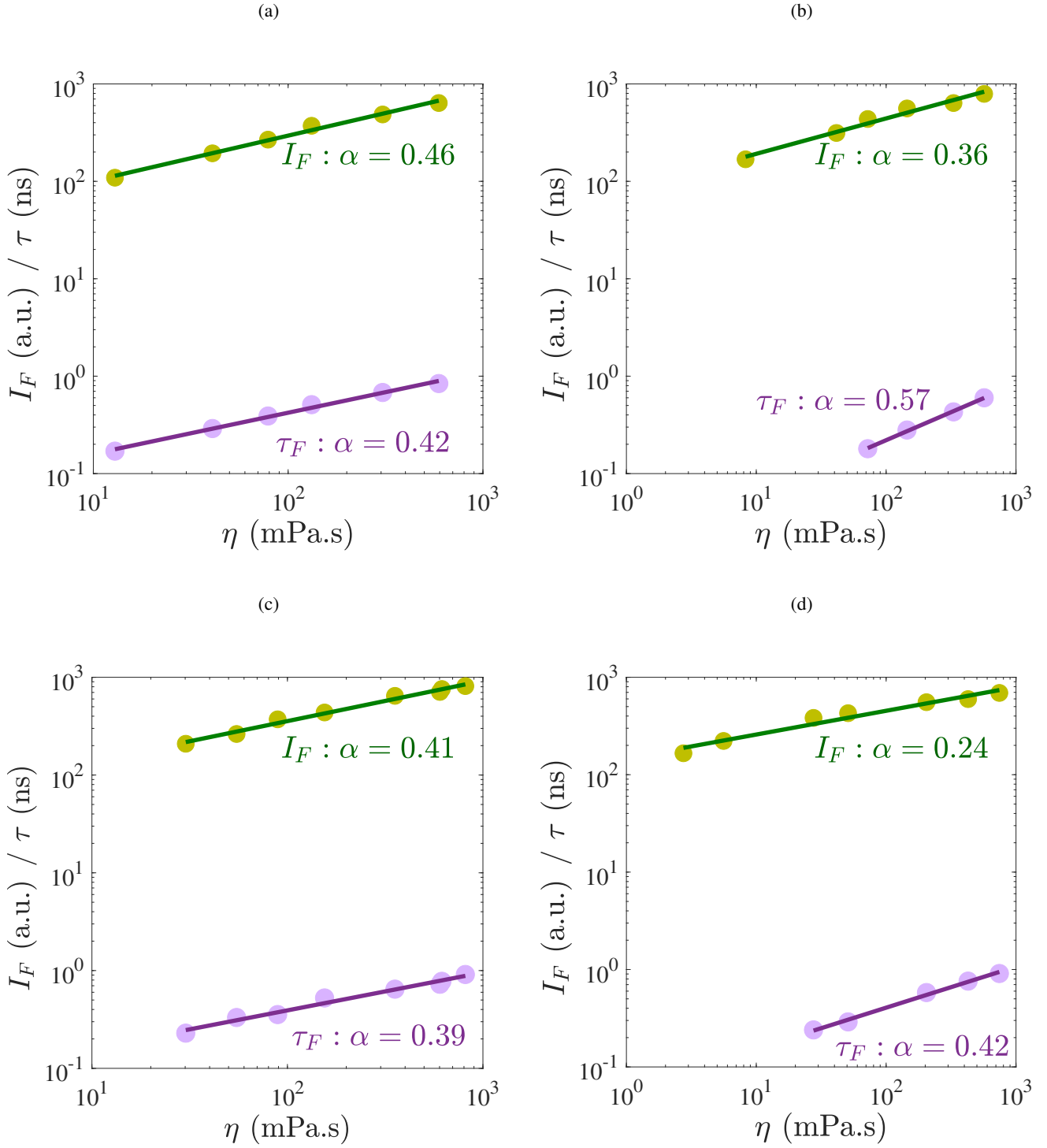


FIG. 11: Calibration curves in logarithmic scale of (a) P1, (b) P2, (c) P3, and (d) P4. I_F values are represented with green points and τ_F with purple points.

tests, with the total duration lasting almost 3 hours, showing the good stability of the microfluidic device. A video obtained during the injection of the different solutions is presented as Supporting Information. Values of the α coefficient of the

Förster-Hoffman relationship were obtained for the different tests performed with different polymer-grafted chips and had a mean value of 0.084, as shown in Figure 16b. The values of α for various viscosity-sensitive surfaces, grafted with polymer

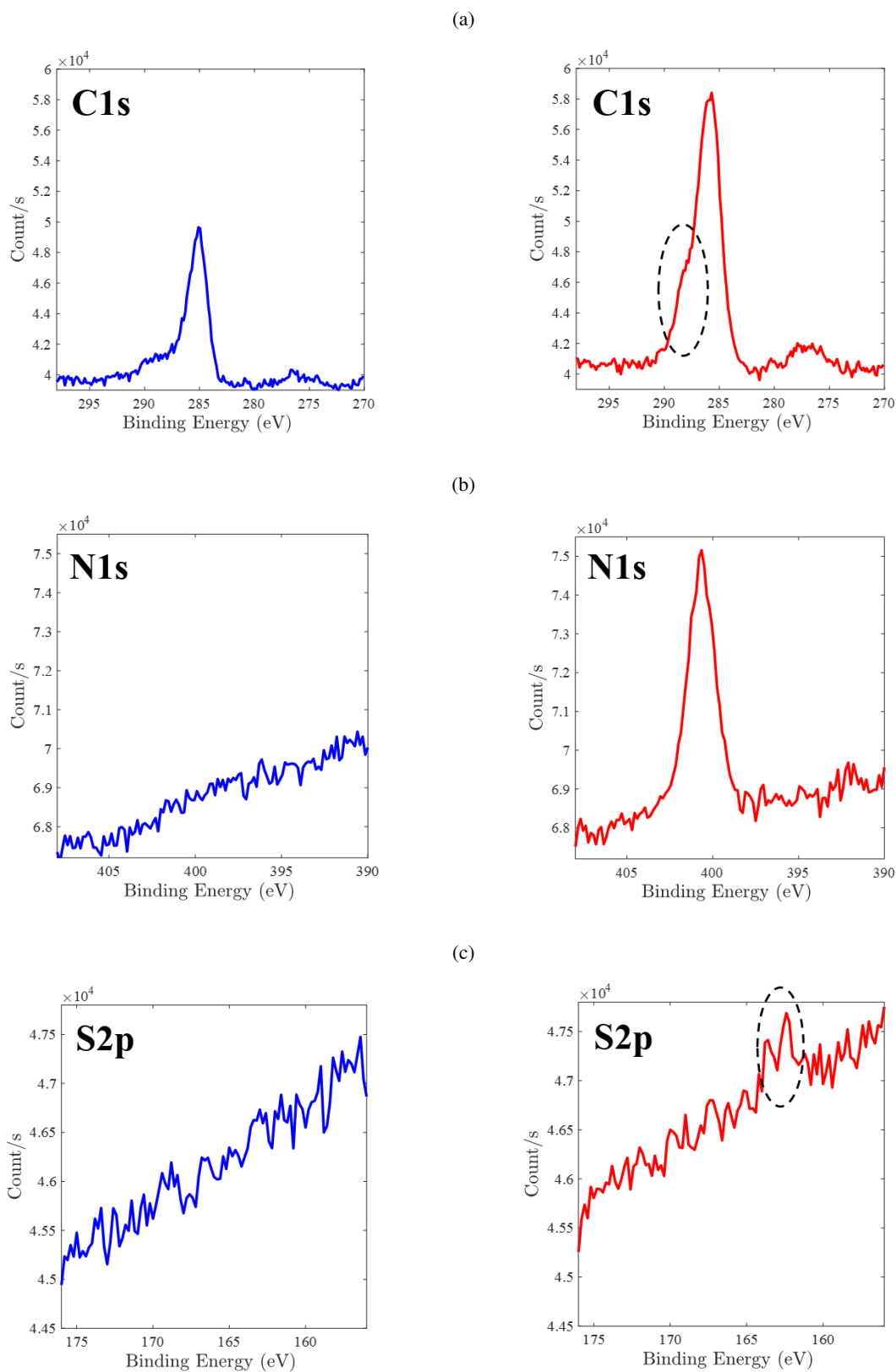


FIG. 12: XPS spectroscopy analysis of a non-grafted gold glass slide (in blue) and of grafted poly(DMA-*s*-MECVJ) on a gold-coated glass slide (in red). (a) Representative C 1s spectrum. (b) Representative N 1s spectrum. (c) Representative S 2p spectrum. The significance of the dashed lines is explained in the accompanying text.

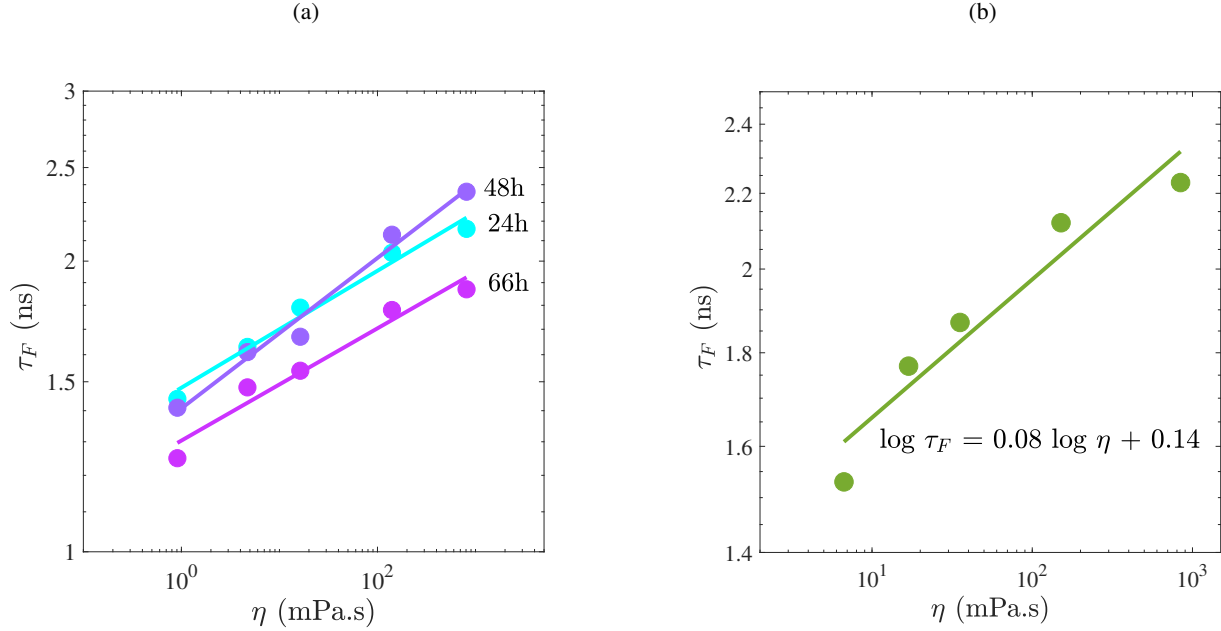


FIG. 13: (a) Fluorescence lifetime response of grafted viscosity-sensitive polymer to mixtures of different viscosity for various grafting times. Solid lines correspond to fit along Eq. (3). (b) Fluorescence lifetime response of grafted viscosity-sensitive polymer to mixtures of different viscosity after continuous washing for 63 hours. Data are plotted in logarithmic scale with η expressed in mPas and τ_F in ns. The straight line represents the Förster-Hoffmann model fit of Eq. (3).

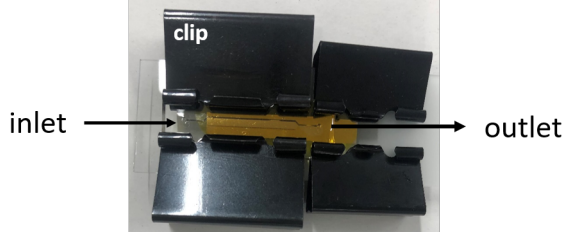


FIG. 14: Photograph of the viscosity-sensitive PDMS microfluidic chip (see schematics on Fig. 3). Length of the field of view is about 8 cm.

solutions of different concentrations and several grafting durations confirm the reproducibility of the results and stable sensitivity to viscosities. The values for α obtained in this work are comparable with and also more reproducible than those obtained in previous studies [33]. As well, the polymeric material reported in this work may exhibit better sensitivity to viscosity than the materials published previously even after grafting onto glass surfaces. It is to note that Kwak's group obtained molecular-rotors grafted polymers with good sensitivity to viscosity and developed polymeric films with proved response to viscosity, however no grafting onto surfaces was performed by this group. [34–36]

IV. CONCLUSIONS AND PERSPECTIVES

Viscosity-sensitive FMRs were successfully integrated into polymeric materials, namely poly(DMA-*s*-MECVJ) by previously synthesizing a viscosity-sensitive monomer called MECVJ and incorporating it during the polymerization. The obtained materials, monomer and polymer, kept the sensitivity to viscosity from the julolidine group. These polymeric materials were successfully anchored onto glass surfaces previously coated with a thin gold film. The surfaces thus obtained were sensitive to the viscosity of fluids flowing through a microchannel fabricated with the polymer-anchored surfaces.

While the polymeric surface presented less sensitivity to the viscosity of the surrounding fluid than the monomer alone, these materials were still useful to fabricate robust viscosity-sensitive surfaces and be used in a micro-channel to obtain a measurement device capable to map the viscosity of a fluid flowing inside the microchannel.

This work represents a step towards the fabrication of viscosity-sensitive polymeric materials where fluorescence lifetime and intensity are related to the viscosity of the fluid in contact. Other polymers could be considered to give flexibility to the polymer chain and maintain the sensitivity of the rotor, or even to optimize the anchoring.

ACKNOWLEDGMENTS

The research presented in this article was funded by the ANR grant MicroVISCOTOR (ANR-18-CE42-0010-01) and

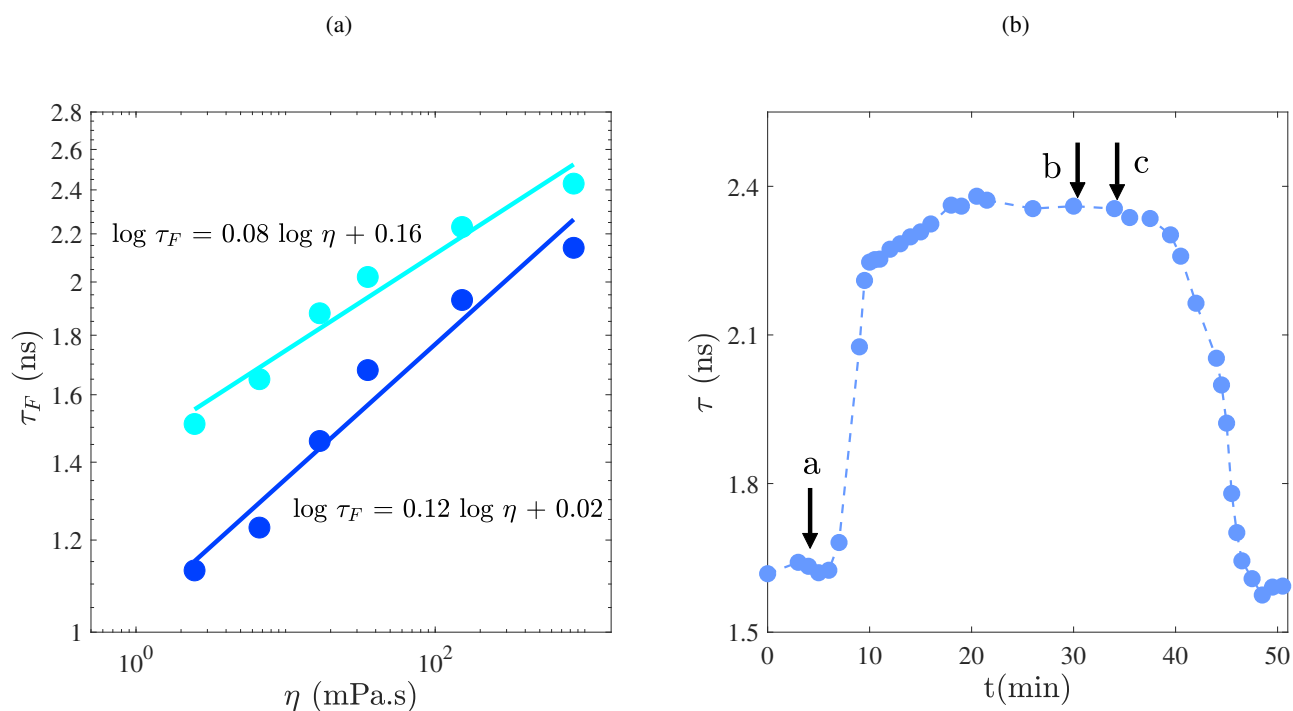


FIG. 15: (a) Calibration curves in logarithmic scale of fluorescence lifetimes, τ_F in two different poly(DMA-*s*-MECVJ)-grafted microfluidic chips versus water-glycerol mixture viscosity, η . The straight lines correspond to fits with the Förster-Hoffmann model with similar coefficient $\alpha \approx 0.1$ for both microdevices when η is expressed in mPa.s and τ_F in ns. (b) Real-time fluorescence response of viscosity-sensitive microfluidic chip developed in this thesis to changes in viscosity; a further explanation on points (a,b, and c) is provided in the accompanying text.

by the MIELS project funded by the Nouvelle Aquitaine Region (project n° 205086). PLACAMAT facility is acknowledged for XPS analysis. Pr. J-C. Barret and Dr. J. Yuan from the CRPP and Dr. B. Cabannes-Boué from the LCPO are thanked for the metallization of glass slides. The authors also thank Solvay and CNRS for funding.

Appendix A: Synthesis of the Julolidine Aldehyde

$^1\text{H-NMR}$ spectra of julolidine (1) and of julolidine aldehyde (2) are provided on Fig. 17.

Appendix B: Synthesis of the viscosity-sensitive monomer (MECVJ)

$^1\text{H-NMR}$ spectra of the synthesized viscosity-sensitive fluorescent monomer MECVJ are provided on Fig. 18.

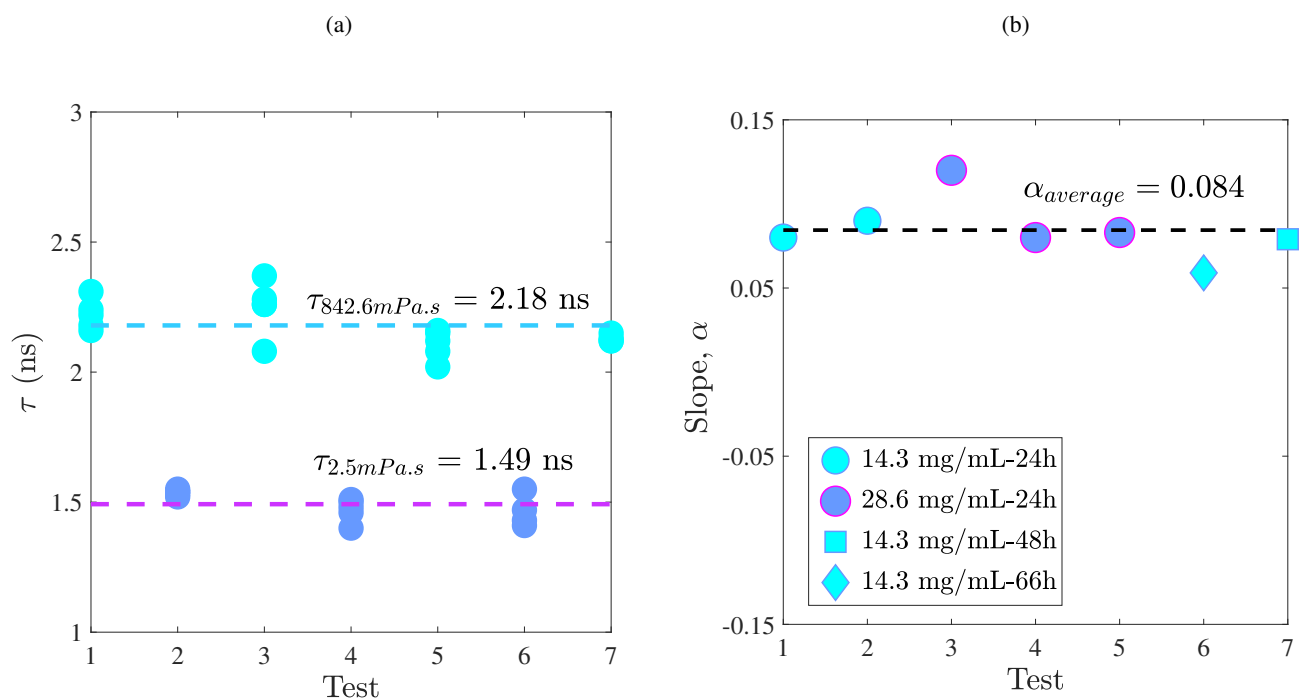


FIG. 16: (a) A plot of fluorescence lifetime values obtained for two different mixtures of glycerol-water tested multiple times on the poly(DMA-*s*-MECVJ)-grafted surface. The average lifetime values for both mixtures are represented by the dotted lines.

(b) Comparison of coefficient- α of the Förster-Hoffmann model (slope-value) obtained for a polymer-grafted surface. The dotted line represents the average value of α for all the represented data.

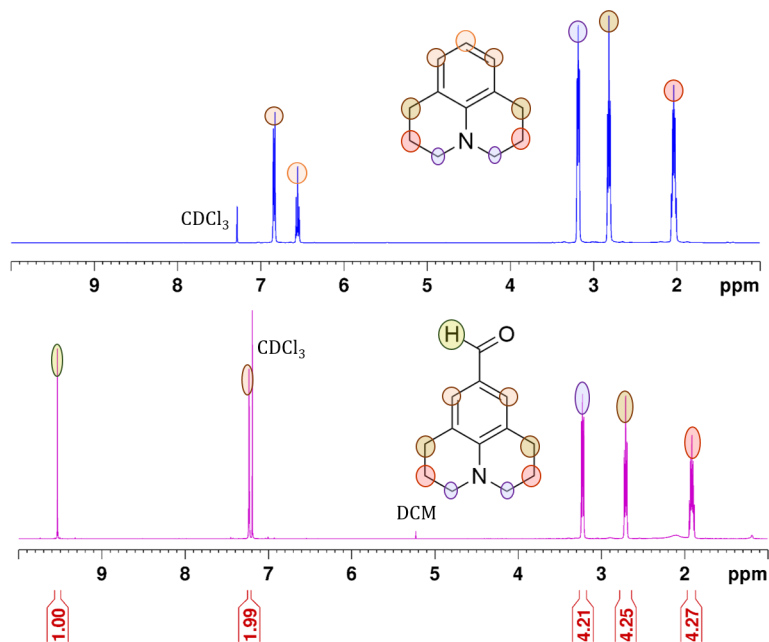


FIG. 17: $^1\text{H-NMR}$ spectra of julolidine (1) and of julolidine aldehyde (2)

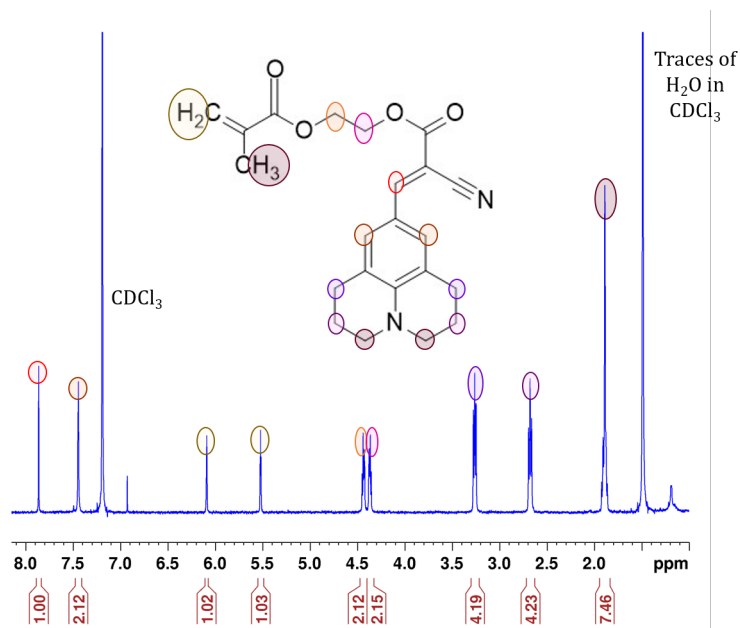


FIG. 18: ¹H-NMR spectrum of viscosity-sensitive monomer, MECVJ.

- cations for complex reactions, *Chemical Engineering Journal* **403**, 126300 (2021).
- [2] C. Meffan, J. Menges, D. Mak, F. Dolamore, F. Conan, N. Volker, and R. C. J. Dobson, Capillary-based micro-optofluidic viscometer, *Sensors and Actuators A: Physical* **359**, 114497 (2023).
- [3] T. Dietrich, A. Freitag, and U. Schlecht, New micro viscosity sensor—a novel analytical tool for online monitoring of polymerization reactions in a micro reaction plant, *Chemical Engineering Journal* **160**, 823 (2010).
- [4] L. Fan, Q. Zan, X. Wang, X. Yu, S. Wang, Y. Zhang, Q. Yang, W. Lu, S. Shuang, and C. Dong, A mitochondria-targeted and viscosity-sensitive near-infrared fluorescent probe for visualization of fatty liver, inflammation and photodynamic cancer therapy, *Chemical Engineering Journal* **449**, 137762 (2022).
- [5] R. Li, J. Guo, Y. Duan, X. Liu, L. Gui, Y. Xu, X. Kong, Y. Li, H. Chen, and Z. Yuan, Monitoring inflammation-cancer progression by cell viscosity, polarity and leucine aminopeptidase using multicolor fluorescent probe, *Chemical Engineering Journal* **435**, 135043 (2022).
- [6] W.-N. Wu, Y.-F. Song, X.-L. Zhao, Y. Wang, Y.-C. Fan, Z.-H. Xu, and T. D. James, Multifunctional 1,3-benzoxazole-merocyanine-based probe for the ratiometric fluorescence detection of $\text{pH}/\text{hso}_3^-/\text{viscosity}$ in mitochondria, *Chemical Engineering Journal* **464**, 142553 (2023).
- [7] T. V. Nguyen, M. D. Nguyen, H. Takahashi, K. Matsumoto, and I. Shimoyama, Viscosity measurement based on the tapping-induced free vibration of sessile droplets using MEMS-based piezoresistive cantilevers, *Lab on a Chip*, 3670 (2015).
- [8] I. Puchades and L. F. Fuller, A thermally actuated microelectromechanical (MEMS) device for measuring viscosity, *Journal of Electromechanical Systems*, 601 (2011).
- [9] S. Kuenzi, E. Meurville, E. Grandjean, S. Straessler, and P. Ryser, Contactless rotational concentric microviscometer, *Sensors and Actuators A*, 194 (2011).
- [10] A. Bamshad, A. Nikfarjam, and H. Sabour, Mohammad, Capillary-based micro-optofluidic viscometer, *Measurement Science and Technology*, 095901 (2018).
- [11] M. Kuimova, A. Vyšniauskas, I. López-Duarte, N. Duchemin, T. Vu, Y. Wu, E. Budykina, Y. Volkova, E. Cabrera, and D. Ramírez-Ornelas, Exploring viscosity, polarity and temperature sensitive of BODIPY-based molecular rotors, *Phys. Chem. Chem. Phys.* **19**, 25252 (2013).
- [12] D. Nalatamby, F. Gibouin, J. Ordóñez-Hernández, J. Renaudeau, G. Clisson, N. Farfán, P. Lidon, and Y. Medina-Gonzalez, Capillary-based micro-optofluidic viscometer, *Industrial & Engineering Chemistry Research* **32**, 12656 (2023).
- [13] M. A. Haidekker and E. A. Theodorakis, Ratiometric mechanosensitive fluorescent dyes: Design and applications, *Journal of Materials Chemistry C* **4**, 2707 (2016).
- [14] F. Gibouin, D. Nalatamby, P. Lidon, and Y. Medina-Gonzalez, Molecular rotors for in situ viscosity mapping during evaporation of confined fluid mixtures, *ACS Appl. Mater. Interfaces* **16**, 8066–8076 (2024).
- [15] M. K. Kuimova, Mapping viscosity in cells using molecular rotors, *Physical Chemistry Chemical Physics* **14**, 12671 (2012).
- [16] S. Strickler and R. A. Berg, Relationship between Absorption Intensity and Fluorescence Lifetime of Molecules, *J. Chem. Phys.* **37**, 814 (1962).
- [17] M. A. Haidekker and E. A. Theodorakis, Molecular rotors - Fluorescent biosensors for viscosity and flow, *Organic and Biomolecular Chemistry* **5**, 1669 (2007).
- [18] M. A. Haidekker and E. A. Theodorakis, Environment-sensitive behavior of fluorescent molecular rotors, *Journal of Biological Engineering* **4**, 1 (2010).
- [19] J. M. Nölle, C. Jüngst, A. Zumbusch, and D. Wöll, Monitoring of viscosity changes during free radical polymerization using fluorescence lifetime measurements, *Polymer Chemistry* **5**, 2700 (2014).
- [20] E. Mirzahosseini, M. Grzelka, Z. Pan, B. Demirkurt, M. Habibi, A. M. Brouwer, and D. Bonn, Molecular rotors to probe the local viscosity of a polymer glass, *The Journal of Chemical Physics* **156**, 174901 (2022).
- [21] M. A. Haidekker, W. J. Akers, D. Fischer, and E. A. Theodor-

- akis, Optical fiber-based fluorescent viscosity sensor, *Optics letters* **31**, 2529 (2006).
- [22] M. A. Haidekker, T. Ling, M. Anglo, H. Y. Stevens, J. A. Frangos, and E. A. Theodorakis, New fluorescent probes for the measurement of cell membrane viscosity, *Chemistry and Biology* **8**, 123 (2001).
- [23] M. Tsakos, E. S. Schaffert, L. L. Clement, N. L. Villadsena, and T. B. Poulsen, Ester coupling reactions – an enduring challenge in the chemical synthesis of bioactive natural products, *Natural Products Reports* **32**, 605 (2015).
- [24] R. O. Loutfy, Fluorescence probes for polymer free-volume, *Pure Appl. Chem* **58**, 439 (1986).
- [25] A. S. Duwez, P. Guikllket, C. Colard, J.-F. Gohy, and C.-A. Fustin, Dithioesters and trithiocarbonates as anchoring groups for the grafting-to approach, *Macromolecules* **39**, 2729 (2006).
- [26] C. E. Kung and K. Jutta, Microviscosity Measurements of Phospholipid Bilayers Using Fluorescent Dyes That Undergo Torsional Relaxation, *Biochemistry* **25**, 6114 (1986).
- [27] M. A. Haidekker, N. L'Heureux, and J. A. Frangos, Fluid shear stress increases membrane fluidity in endothelial cells: a study with dcvj fluorescence, *American Journal of Physiology-Heart and Circulatory Physiology* **278**, 1401 (2000).
- [28] G. Moad and S. H. Thang, Raft polymerization and some of its applications, *Chem. Asian J.* **8**, 1634 (2013).
- [29] F. Ercole, N. Malic, S. Harrisson, T. P. Davis, and R. A. Evans, Photochromic polymer conjugates: the importance of macromolecular architecture in controlling switching speed within a polymer matrix, *Macromolecules* **43**, 249 (2010).
- [30] N. T. Trang, S. Maiez-Tribut, J.-P. Pascault, A. Bonnet, P. Gerard, O. Guerret, and D. Bertin, Synthesis and characterizations of block copolymer of poly(n-butyl acrylate) and gradient poly(methyl methacrylate-co-n,n-dimethyl acrylamide) made via nitroxide-mediated controlled radical polymerization, *Macromolecules* **40**, 4516 (2007).
- [31] A. B. Lutjen, M. A. Quirk, and E. M. Kolonko, Synthesis of esters via a greener stepwise esterification in acetonitrile, *J. Vis. Exp.*, e58803 (2018).
- [32] C.-A. Fustin and A.-S. Duwez, Dithioesters and trithiocarbonates monolayers on gold, *J. Electron Spectrosc. Relat. Phenom.* **172**, 104 (2009).
- [33] D. J. Lichlyter and M. A. Haidekker, Immobilization techniques for molecular rotors—towards a solid-state viscosity sensor platform, *Sensors and Actuators, B: Chemical* **139**, 648 (2009).
- [34] W.-E. Lee, C.-L. Lee, T. Sakaguchi, M. Fujiki, and G. Kwak, Fluorescent viscosity sensor film of molecular-scale porous polymer with intramolecular π -stack structure, *Macromolecules* **44**, 432 (2011).
- [35] Y.-J. Jin, H. Park, Y.-J. Ohk, and G. Kwak, Hydrodynamic fluorescence emission behavior of molecular rotor-based vinyl polymers used as viscosity sensors, *Polymer* **132**, 79 (2017).
- [36] Y.-J. Jin, Y.-G. Choi, and G. Kwak, Thermodynamic and hydrodynamic fluorescence emission behaviors of polydiphenylacetylenes with different size of substituents, *Polymer* **171**, 127 (2019).